

# Excitation Transport and Trapping in a Synthetic Chlorophyllide Substituted Hemoglobin: Orientation of the Chlorophyll $S_1$ Transition Dipole<sup>†</sup>

Richard S. Moog, Atsuo Kuki, M. D. Fayer, and Steven G. Boxer\*

**ABSTRACT:** Excitation transport in synthetic zinc chlorophyllide substituted hemoglobin has been observed by pico-second time-resolved fluorescence depolarization experiments. In this hybrid molecular system, two zinc chlorophyllide molecules are substituted into the  $\beta$ -chains of hemoglobin, while deoxy hemes remain in the  $\alpha$ -chains. The rate of excitation transfer between the two chlorophyllides is analyzed in terms of the distance and orientation dependences predicted by the Förster dipole-dipole theory. In this analysis, the  $\beta$ - $\beta$  interchromophore geometry is assumed to be that of the deoxyhemoglobin crystal structure. When combined with

steady-state fluorescence depolarization data of the complementary hybrid containing zinc chlorophyllide in the  $\alpha$ -chains, these experiments provide the necessary information to determine the orientation of the  $S_1$  transition dipole moment in the zinc chlorophyllide molecule. We also find that the fluorescence lifetime of the zinc chlorophyllide is 1.42 ns when the heme is in the deoxy state but 3.75 ns when the heme is ligated to carbon monoxide. This is explained by irreversible excitation transfer from the  $S_1$  state of the zinc chlorophyllide to the lower energy excited states present in deoxy heme.

The substitutional incorporation of a chlorophyllide molecule into a host protein, combined with polarized spectroscopy, permits the observation of the oriented properties of the chromophore (Boxer et al., 1982). We present a time-resolved investigation of the orientation-dependent excitation transfer between the lowest singlet excited states ( $S_1$  states) of two chlorophyllides specifically inserted into the same protein molecule. This synthetic molecular system was selected to allow the determination of the orientation of the transition dipole moment for the  $S_1$  state relative to the chlorophyll molecular frame and to investigate the effect of the protein environment on the excitation transfer process. The orientation of the transition dipole is the cornerstone of all interpretations of polarized light spectroscopy, excitonic interactions, or resonance excitation transfer in natural chlorophyll-containing systems in terms of their molecular architecture.

The transport of singlet excitation has been observed and studied in many polychromophoric systems. Random solutions (Gochanour & Fayer, 1981; Miller et al., 1983), micelles (Koglin et al., 1981; Ediger et al., 1984), monolayers (Tweet et al., 1964; Trosper et al., 1968), polymers (Stryer & Haugland, 1967; Seely, 1970), and naturally occurring proteins (Fairclough & Cantor, 1978) have all been subject to such investigations. In general these systems exhibit interchromophore distances and relative orientations which are either random, fluctuating, or unknown. Proteins are the exception, as they possess specific binding sites for their chromophores. The reconstitution of human semihemoglobins with two chlorophyllides takes advantage of this aspect of protein structure, providing a system of two chromophores separated

by a sufficient distance so that exchange and excitonic interactions are absent (Kuki & Boxer, 1983). The well-defined tertiary and quaternary structure of the hemoglobin (Hb)<sup>1</sup> molecule ensures that the relative orientation of each interacting pair of chlorophyllides is constant.

Previous work has shown that various chlorophyllides and zinc bacteriochlorophyllide *a* can be reconstituted into the heme pocket of apomyoglobin (apoMb) and that the binding is specific (Wright & Boxer, 1981). Zinc pyrochlorophyllide *a* (ZnPChla; Figure 1) also inserts specifically into the four heme pockets of human apohemoglobin (apoHb) and into the two empty heme pockets of semihemoglobin prepared with either  $\alpha$ - or  $\beta$ -pockets retaining the native heme group. The resulting hybrid protein containing deoxy hemes in the  $\alpha$ -chains and ZnPChla in the  $\beta$ -chains,  $\alpha_2^h(\text{deoxy})\beta_2^{\text{Chl}}$  (Figure 2), and the complementary hybrid  $\alpha_2^{\text{Chl}}\beta_2^h(\text{deoxy})$  are both tightly associated as  $\alpha_2\beta_2$  tetramers (Kuki & Boxer, 1983). The tertiary and quaternary structures of these proteins were shown by a variety of tests to be very similar to that of the native deoxy-Hb, whose crystal structure is known. Possessing exactly two chlorophylls, and hence only one interfluorophore excitation transfer rate constant, these hybrids are the structures of choice for a time-resolved investigation.

The protein  $\alpha_2^h(\text{deoxy})\beta_2^{\text{Chl}}$ , which is analyzed fully here, possesses an interfluorophore center-to-center separation of 40.2 Å. At 40 Å, the interaction energy of the two chlorophyll transition dipoles is such that excitation transfer is expected to occur with a characteristic time in the neighborhood of 1.5 ns. The exact value of the interaction energy, and hence of the transfer rate constant, is naturally dependent on the mutual orientation of the two transition dipoles. In this paper, this orientational dependence is used to determine the direction of the chlorophyllide  $S_1$  transition dipole moment. The  $S_1$  transition is also known as the  $Q_Y$  (peak wavelength ~660 nm) as theoretical calculations predict an approximately *Y* orientation.

The two chlorophyllides in the  $\beta$ -chains are related by a  $C_2$  symmetry axis; thus, not only the chromophores but also their environments are identical. It follows that the product of a

<sup>†</sup> From the Department of Chemistry, Stanford University, Stanford, California 94305. Received September 15, 1983. This work was supported by grants from the National Science Foundation (PCM8303776), the Gas Research Institute (GRI-5083-260-0824), (S.G.B.) and the U.S. Department of Energy, Office of Basic Energy Sciences (DE-AT03-82ER12055) (M.D.F.). The National Science Foundation (DMR79-20380) is also acknowledged for providing and supporting equipment necessary for this research (M.D.F.). Some fluorescence lifetimes were obtained at the Stanford Synchrotron Radiation Laboratory supported by National Institutes of Health Grant 01209. M.D.F. would like to acknowledge the Simon Guggenheim Memorial Foundation for fellowship support which contributed to this research. S.G.B. is an Alfred P. Sloan and Camille and Henry Dreyfus Teacher-Scholar Fellow.

<sup>1</sup> Abbreviations: Hb, hemoglobin; Mb, myoglobin; ZnPChla, zinc pyrochlorophyllide *a*; FWHM, full width at half-maximum.

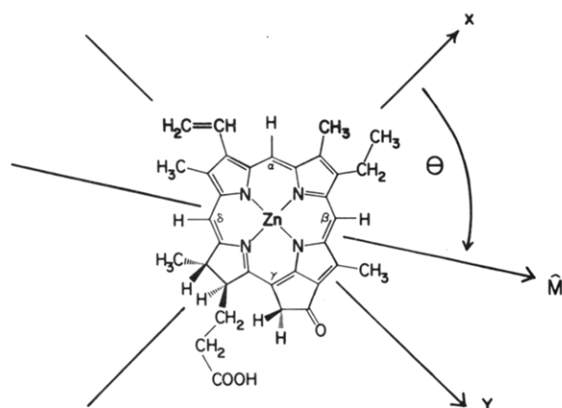


FIGURE 1: Structure of zinc pyrochlorophyllide *a* molecule. By convention, the coordinate system of *X* and *Y* in-plane axes is as depicted.  $\hat{M}$  denotes the unit vector of the transition dipole moment for the lowest excited singlet state.

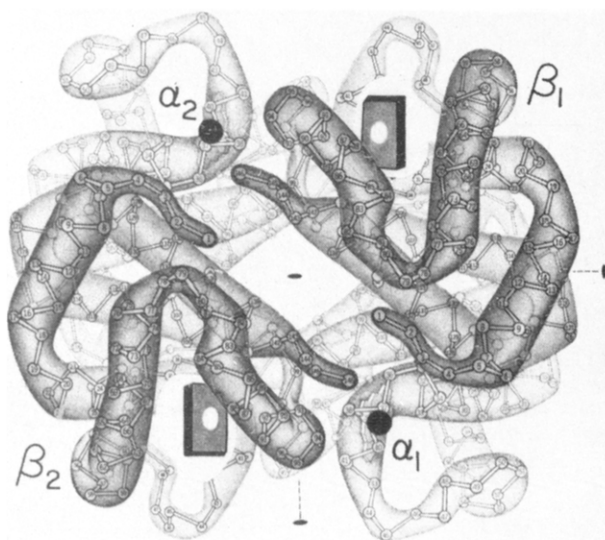


FIGURE 2: Depiction of the hemoglobin hybrid containing two chlorophyllides and two hemes,  $\alpha_2^h(\text{deoxy})\beta_2^{\text{chl}}$ . The square planes with white centers in the  $\beta$ -chains represent ZnPCChla and the heavy black dots in the  $\alpha$ -chains represent the centers of the hemes. Adapted from Dickerson & Geis (1969).

chlorophyll–chlorophyll excitation transfer event will be indistinguishable from the reactant in almost all respects. The transfer process can be observed, however, by the well-known method of fluorescence depolarization in the viscous solution limit, where rotational relaxation is negligible (Albrecht, 1961; Dale & Eisinger, 1975). The anisotropy of the fluorescence is monitored following direct excitation of the chlorophyllide  $S_1$  state with a pulse of linearly polarized light. The fluorescence anisotropy,  $r(t)$ , is defined as

$$r(t) = \frac{I_{\parallel}(t) - I_{\perp}(t)}{I_{\parallel}(t) + 2I_{\perp}(t)} \quad (1)$$

where  $I_{\parallel}(t)$  and  $I_{\perp}(t)$  are equal to the intensity of fluorescence observed through an emission polarizer oriented parallel and perpendicular, respectively, to the direction of polarization of the exciting pulse (Jablonski, 1961). At the moment of the exciting flash, only originally photoselected chromophores fluoresce, and the emission anisotropy is at its maximum value, the monomer anisotropy ( $r_0$ ). The anisotropy then degrades in time by an exponential decay governed by the rate of the intraprotein excited-state population transfer to the other, originally unexcited, chromophore (Figure 3). At a time sufficiently long so that the excited-state population has

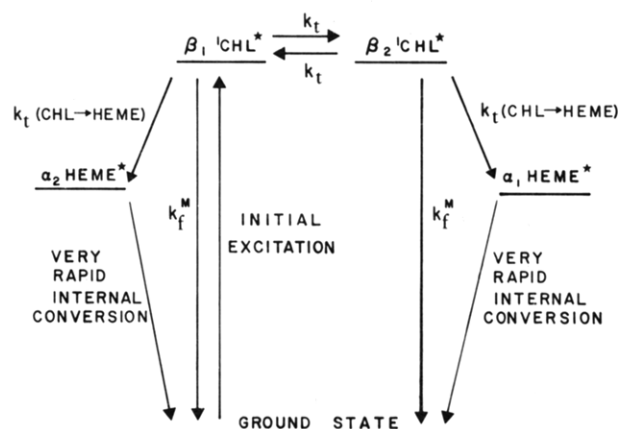


FIGURE 3: Kinetic scheme for the processes following excitation into the  $S_1$  state of a single chlorophyllide in the  $\alpha_2\beta_2^{\text{chl}}$  complex.  $k_f^M$  is the observed fluorescence decay rate for monomeric ZnPCChlaMb ( $2.6 \times 10^8 \text{ s}^{-1}$ ) and includes radiative decay, internal conversion, and intersystem crossing. The fluorescence lifetime observed in the hybrids is  $\tau_f = (k_f)^{-1} = [k_f^M + k_t(\text{Chl} \rightarrow \text{heme})]^{-1}$ .

equilibrated between the two fluorophores, a characteristic nonzero emission anisotropy,  $r_{\infty}$ , is observed.

That the time-resolved emission anisotropy is expected to have the theoretical form of an exponential decay to a nonzero base line can be understood as follows.  $\hat{M}_1$  and  $\hat{M}_2$  are defined as the principal normalized transition dipoles for the fluorescent transition on the originally excited chlorophyllide and the chlorophyllide in the other  $\beta$ -chain, respectively. An intraprotein excitation transfer event resulting in fluorescence from  $\hat{M}_2$  will reduce the emission anisotropy below the monomer value to the extent that the dot product  $\hat{M}_1 \cdot \hat{M}_2$  is less than one. When  $r_{1 \rightarrow 2}$ , the transfer anisotropy, is defined as the anisotropy of emission from the chromophore not initially excited, it is straightforward to show (Tao, 1969) that

$$r_{1 \rightarrow 2} = (2/5)P_2(\hat{M}_1 \cdot \hat{M}_2) \quad (2)$$

where  $P_2$  is the second Legendre polynomial.

The emission anisotropy of a sample of  $\alpha_2^h(\text{deoxy})\beta_2^{\text{chl}}$  is given at any time by the population weighted average of the monomer and transfer anisotropies:

$$r(t) = \frac{p_1(t)r_0 + p_2(t)r_{1 \rightarrow 2}}{p_1(t) + p_2(t)} \quad (3)$$

Following a  $\delta$ -function excitation, the excited-state populations of the originally excited fluorophore,  $p_1(t)$ , and of the originally unexcited fluorophore,  $p_2(t)$ , are given by (see Figure 3)

$$\begin{aligned} p_1(t) &= (1/2)[1 + \exp(-2k_t t)] \exp(-k_f t) \\ p_2(t) &= (1/2)[1 - \exp(-2k_t t)] \exp(-k_f t) \end{aligned} \quad (4)$$

where  $k_t$  is the rate constant for excitation transfer and  $k_f$  is the rate constant for the decay of the singlet excited state. Inserting these expressions into eq 3 yields

$$r(t) = (1/2)(r_0 - r_{1 \rightarrow 2}) \exp(-2k_t t) + (1/2)(r_0 + r_{1 \rightarrow 2}) \quad (5)$$

from which we can make the identification  $r_{\infty} = (1/2)(r_0 + r_{1 \rightarrow 2})$ .

The significant feature of the fluorescence anisotropy experiment is that both  $r_{\infty}$  and  $k_t$  contain information about the relative orientation of the lowest energy singlet transition dipole moment. We also find that the deoxy heme chromophores 25 Å away in the  $\alpha$ -chains serve unexpectedly as excitation traps, shortening the fluorescence lifetime of ZnPCChla. The effectiveness of this excitation trapping is studied as a function of the state of the heme group.

### Experimental Procedures

The hybrid chlorophyllide-substituted hemoglobins were synthesized as described previously (Kuki & Boxer, 1983).

The time-resolved fluorescence depolarization measurements were made by using the fluorescence mixing technique (Gochanour & Fayer, 1981; Ediger et al., 1984). The 1.06- $\mu\text{m}$  output of a continuously pumped acousto-optically Q-switched and mode-locked Nd:YAG laser was frequency doubled, and the 532-nm component was used to synchronously pump a DCM dye laser at 400 Hz. The dye laser was cavity dumped, providing a single pulse of less than 50 ps (FWHM) at 660 nm. This output was used to excite the sample, after appropriate attenuation to avoid deviations from a  $\cos^2$  initial excitation distribution. The onset of nonlinear excitation was easily detected as a decrease in the anisotropy of monomeric samples. At the excitation intensity used, most protein molecules have zero excitation, a small number have a single excitation, and effectively zero have both chlorophyllides excited. The resulting fluorescence was isolated from scattered light with a narrow band interference filter ( $\lambda_{\text{max}}$  672 nm, FWHM = 10 nm) and focused into an RDP type I sum generating crystal. A single IR laser pulse (FWHM = 125 ps) was selected from the IR pulse train by a Pockels cell and also focused into the crystal. Fluorescence reaching the crystal time-coincident with the 1.06- $\mu\text{m}$  pulse produced a short burst of light at 410 nm. This signal was isolated by a series of filters and detected by a photomultiplier tube (EMI 6256) and lock-in. The summing crystal was oriented so that only the component of the sample fluorescence polarized parallel to the 1.06- $\mu\text{m}$  polarization was summed. A half-wave plate was placed in the path of the 660-nm excitation beam so that the polarization of the excitation pulse could be set parallel, perpendicular, or at the magic angle relative to the IR pulse. This apparatus yields an emission anisotropy for Oxazine 725 in glycerol of 0.39. The decay obtained at magic angle polarization [ $I_M(t)$ ] was used to determine the fluorescence lifetimes.

The time evolution of the fluorescence anisotropy was obtained by examining the polarized fluorescence intensities as a function of the delay between the arrival of the excitation pulse at the sample and the arrival of the IR pulse at the summing crystal. Data were obtained on several samples at a number of different delays. At a given position all three polarizations were measured successively by averaging each signal for 30 s. The sum

$$S(t) = (1/3)[I_{\parallel}(t) + 2I_{\perp}(t)] \quad (6)$$

was performed and compared to  $I_M(t)$  for each time point; the data were accepted only if the two values were identical within the uncertainty.

The deoxygenated protein samples were prepared by reducing a degassed stock solution of  $\alpha_2^{\text{h}}(\text{cyanomet})\beta_2^{\text{chl}}$  with sodium dithionite and subsequent dilution with a degassed sucrose solution in 10 mM sodium phosphate, pH 7.0. The final concentration of sucrose was 19% (w/total w), and that of the dithionite was 0.05%. The samples were then loaded into a 1-mm path-length absorption cuvette in an inert atmosphere box ( $p\text{O}_2 < 1$  ppm) and sealed. The samples were 37  $\mu\text{M}$  in protein (tetramer) concentration. As the corresponding reduced concentration ( $^4/3\pi R_0^3\rho$ , where  $\rho$  is the molecule number density) is 0.006, interprotein excitation transfer is completely negligible. Reabsorption reemission processes were also negligible as verified by the identical results obtained with protein samples of half this concentration. The absorption spectrum of the sample was monitored throughout each run to ensure that sample degradation was negligible.

The fluorescence lifetimes of  $\alpha_2^{\text{h}}\beta_2^{\text{chl}}$  with the heme in the cyanomet and carbonmonoxy states were obtained by using single-photon counting equipment following excitation at 420 nm with a 400-ps (FWHM) pulse of synchrotron light at the Stanford Synchrotron Radiation Laboratory (Munro et al., 1979; Munro & Sabersky, 1980). An RCA 8852 photomultiplier tube detected the magic angle polarized fluorescence at 90°. The lifetimes were obtained by deconvolution of the synchrotron pulse profile (measured at the detection wavelength, 670 nm) combined with nonlinear least-squares analysis (Shrager, 1970; Grinvald & Steinberg, 1974).

Absorption spectra for  $R_0$  spectral overlap calculations (see Discussion) were taken on a Cary 2300 absorption spectrometer and were stored digitally. The chlorophyllide-protein extinction coefficients were recorded as extinction per chlorophyllide chromophore. The spectra to be used for  $R_0$  calculations were corrected for the presence of the heme moieties in the following manner. An absorption spectrum of deoxy-hemoglobin was recorded and stored in terms of extinction per heme chromophore. This spectrum was then subtracted from the  $\alpha_2^{\text{h}}(\text{deoxy})\beta_2^{\text{chl}}$  spectrum to provide an absorption spectrum due only to the chlorophyllide chromophores in the complex.

Steady-state fluorometry was performed by using a 1 cm quartz cell, with excitation provided by the vertically polarized continuous output of an Ar<sup>+</sup>-pumped R6G dye laser. Cresyl violet, used as a fluorescence quantum yield standard [0.545 in methanol (Magde et al., 1979)], was excited at 568 nm while the chlorophyllide complexes were excited at 610 nm. All samples had an optical density of less than 0.05 at the peak of the red absorption band. In order to ensure constant illumination intensity over the relevant portion of the solution, the laser output was spatially expanded. Fluorescence was collected by a lens at 90° to the excitation direction and was focused through a polarizer at 54.7° from vertical onto the input slits of a Spex 1702  $^3/4$ -m monochromator. Under these conditions the  $1/n^2$  index of refraction correction for quantum yields is appropriate (Ediger et al., 1982). These spectra were corrected by comparison to the spectrum obtained from the output of a secondary-standard black body lamp. The intensity of light used to excite the sample was monitored by a Scientech power meter and was constant to within  $\pm 0.5\%$  over the time of a fluorescence scan.

### Results

The results of the time-resolved measurements are presented in Figure 4. Each data point is the average of three to seven anisotropy determinations. The error bars represent corresponding standard deviations. The data have been corrected for minor rotational motion with a correlation time of 48 ns,<sup>2</sup> so that only the decay of anisotropy caused by excitation transfer is depicted. The anisotropy decay has the form of an exponential decay to a *nonzero* base line, as anticipated for this system. The theoretical curves for the anisotropy decay (in the limit of  $\delta$ -function excitation) depend on the two parameters  $k_t$  and  $r_{\infty}$  as follows:

$$r(t) = (r_0 - r_{\infty}) \exp(-2k_t t) + r_{\infty} \quad (7)$$

The experimental anisotropy decay was fit to theoretical curves which included convolution with excitation and detection pulse

<sup>2</sup> The observed rotational relaxation time for Hb in water at 20 °C is 26 ns (McCalley et al., 1972), which is in full agreement with the prediction of the Stokes-Einstein equation for a spherical macromolecule with a hydrated volume of 110 000 Å<sup>3</sup>. The viscosity of a 19% sucrose solution is 1.86 times that of water at 20 °C, so we expect a rotational relaxation time of 48 ns.

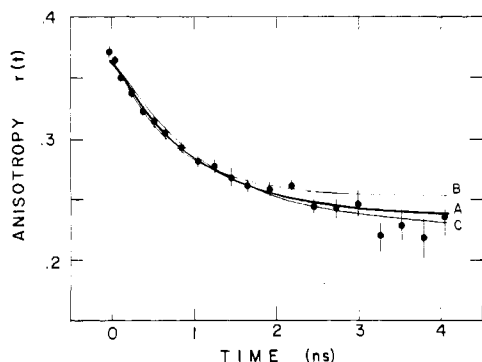


FIGURE 4: Fluorescence anisotropy of  $\alpha_2^h(\text{deoxy})\beta_2^{\text{Chl}}$ . The dots represent the data and are the average of three to seven anisotropy determinations. The error bars are standard deviations of the mean. Theoretical curves A–C, calculated from the deoxy-Hb crystal structure and the scheme shown in Figure 3, cover the range of curves which provide fits to the data (see text). Curve A, for  $\theta = 95.5^\circ$ ,  $z = -3^\circ$ :  $k_t = 5.2 \times 10^8 \text{ s}^{-1}$ ,  $r_\infty = 0.237$ . Curve B, for  $\theta = 32^\circ$ ,  $z = -2^\circ$ :  $k_t = 6.6 \times 10^8 \text{ s}^{-1}$ ,  $r_\infty = 0.253$ . Curve C, for  $\theta = 94^\circ$ ,  $z = -2^\circ$ :  $k_t = 4.2 \times 10^8 \text{ s}^{-1}$ ,  $r_\infty = 0.227$ . All curves are based on  $R_0 = 39.7 \text{ \AA}$ .

Table I: Fluorescence Lifetimes, Quantum Yields, and Values of  $R_0$  for Degenerate Excitation Transfer

	$\tau_f$ (ns)	$R_0$ ( $\text{\AA}$ )	$\eta_f$ (quantum yield)	$\tau_f/\eta_f$ (ns)	$R_0^6/\tau_f^6$ $\times 10^{-18}$ ( $\text{s}^{-1} \text{ \AA}^6$ )
$\alpha_2^h(\text{deoxy})\beta_2^{\text{Chl}}$	$1.42 \pm 0.05$	$39.7 \pm 1.0$	$0.055 \pm 0.005$	$26 \pm 2$	$2.8 \pm 0.4$
ZnPChlaMb	$3.9 \pm 0.2$	$49.1 \pm 0.2$	$0.166 \pm 0.005$	$23.5 \pm 1.4$	$3.6 \pm 0.3$
Chla/Et <sub>2</sub> O	$6.09^a$	58	0.33	18.5	6.25

<sup>a</sup> From Connolly et al. (1982).

shapes.<sup>3</sup> The Fischer *F*-test with 90% confidence limits was used as the fitting criterion. The value of  $r_0$  was restricted to  $0.374 \pm 0.004$ , consistent with the observed value for  $r_0$  for ZnPChlaMb, but the values for  $k_t$  and  $r_\infty$  were freely varying parameters. A few such fits are shown in Figure 4. The curves that fit the data can be described by a region of ( $k_t, r_\infty$ ) space in which the uncertainties in  $k_t$  and  $r_\infty$  are coupled and are not independent. The values of  $k_t$  and  $r_\infty$  within this region range from  $4.0 \times 10^8 \text{ s}^{-1}$  and 0.221, respectively, to  $7.1 \times 10^8 \text{ s}^{-1}$  and 0.252, respectively. Due to the interdependence, however, arbitrary combinations of these two parameters within these ranges do not necessarily provide fits to the data.

The measured values of the fluorescence lifetime,  $\tau_f$ , and the fluorescence quantum yield,  $\eta_f$ , for ZnPChlaMb and  $\alpha_2^h(\text{deoxy})\beta_2^{\text{Chl}}$  are listed in Table I.  $R_0$ , also listed, is the Förster excitation transfer parameter defined below (see eq 10 and Discussion). Note that although both  $\tau_f$  and  $\eta_f$  for the tetrameric deoxy hybrids are less than for the monomer, the radiative lifetime  $\tau_f/\eta_f$  is essentially equal in the two cases. This ZnPChla-protein radiative lifetime is 33% longer than the radiative lifetime for chlorophyll *a* in ethyl ether which is also presented in Table I for comparison.

<sup>3</sup> Since the experimental anisotropies are calculated according to eq 1, theoretical curves for  $I_{\parallel}(t)$  and  $I_{\perp}(t)$  were first convolved with the measured excitation and detection pulse shapes and then combined as in eq 1 to yield the anisotropy decay curves. It is straightforward to show that the corresponding theoretical  $I_{\parallel}(t)$  and  $I_{\perp}(t)$  curves for the case of a resonant chromophore pair are

$$I_{\parallel}(t) = 2C[(1 + 2r_\infty) \exp(-k_t t) + 2(r_0 - r_\infty) \exp[-(k_t + 2k_i)t]]$$

$$I_{\perp}(t) = C[(2 - 2r_\infty) \exp(-k_t t) - 2(r_0 - r_\infty) \exp[-(k_t + 2k_i)t]]$$

where  $C$  is an appropriate constant of proportionality.  $\Delta$

Table II: Dependence of the Chlorophyllide Fluorescence Lifetime on the State of the Heme and Chlorophyll-to-Heme Excitation Transfer Rate Constants and  $R_0$  Values

	$\tau_f$ (ns)	$k_t(\text{Chl} \rightarrow \text{heme})^a$ ( $\text{s}^{-1}$ )	$R_0^b$ ( $\text{\AA}$ )
$\alpha_2^h(\text{deoxy})\beta_2^{\text{Chl}}$	1.42	$4.4 \times 10^8$	25.0
$\alpha_2^h(\text{cyanomet})\beta_2^{\text{Chl}}$	3.19	$4.5 \times 10^7$	20.2
$\alpha_2^h(\text{carbonmonoxy})\beta_2^{\text{Chl}}$	3.75		$\sim 15$
$\alpha_2^{\text{Chl}}\beta_2^{\text{Chl}}$	3.73		

<sup>a</sup> Calculated from the shortening of the lifetime relative to  $\alpha_2^{\text{Chl}}\beta_2^{\text{Chl}}$ . <sup>b</sup> Calculated by using the fluorescence quantum yield in the absence of the heme excitation trapping pathway ( $\eta_f = 0.166$ ).

The dependence of the chlorophyllide fluorescence lifetime on the state of the heme in the hybrid complex is shown in Table II. The lifetime of the fully substituted tetramer  $\alpha_2^{\text{Chl}}\beta_2^{\text{Chl}}$  is equal to that for the monomeric ZnPChlaMb listed in Table I. The lifetimes of the heme-containing complexes, on the other hand, change as the state of the heme is altered, in concert with changes in the  $R_0$  for chlorophyllide-to-heme excitation transfer as calculated from spectral overlap (see below). In order to investigate the possibility of heme-to-chlorophyllide excitation transfer, fluorescence excitation spectra of  $\alpha_2^{\text{Chl}}\beta_2^{\text{Chl}}$  and  $\alpha_2^h(\text{deoxy})\beta_2^{\text{Chl}}$  were measured in the Soret region. The two spectra were essentially identical (within 5% experimental error), confirming, as expected, that there could be no excitation transfer to the chlorophyllides from the hemes.

## Discussion

The dipole character of the chlorophyllide fluorescent transition manifests itself in the orientation dependence of two separate physical interactions: the interaction of the chlorophyllide with polarized light and the interaction of the two chlorophyllides with each other which gives rise to nonradiative excitation transfer. These two interactions will be analyzed in turn. The theoretical predictions for the orientation of the  $Q_y$  transition dipole within the molecular frame are  $\theta = 92^\circ$  (Chang, 1977),  $\theta = 89^\circ$  (Weiss, 1972),  $\theta = \sim 70^\circ$  (Song et al., 1972), and  $\theta = 84.5^\circ$  (Petke et al., 1979) (see Figure 1 for definition of  $\theta$ ). With the advent of the synthetic chlorophyllide substituted proteins (Boxer et al., 1982; Kuki & Boxer, 1983), it became possible to test these predictions experimentally.

**Analysis of the  $r_\infty$  Asymptote.** At a time  $t \gg 1/(2k_i)$  the emission anisotropy of the sample reaches an asymptote,  $r_\infty$ , which is related to the transfer anisotropy by  $r_\infty = (1/2)(r_0 + r_{1 \rightarrow 2})$ . Since the fluorescence lifetime of  $\alpha_2^h(\text{deoxy})\beta_2^{\text{Chl}}$  is anomalously short (1.42 ns) for a zinc pyrochlorophyllide *a* protein, resulting in  $\tau_f \sim 1/(2k_i)$ , the asymptotic anisotropy is best obtained by a curve-fitting analysis of the entire data set to an exponential plus a base line. In fact the curve-fitting analysis (see Results) showed, as one would expect, that the uncertainties in the value of  $r_\infty$  are coupled to the uncertainties in the value of  $k_t$ . For this reason, the final analysis will be done by a simultaneous comparison of ( $k_t, r_\infty$ ) as a function of  $\theta$  with the data.

In Figure 5A the dependence of  $r_{1 \rightarrow 2}$  on  $\theta$ , calculated from the crystal structure coordinates of deoxy-Hb,<sup>4</sup> is displayed.

<sup>4</sup> Deoxyhemoglobin coordinates were obtained at the Computer Graphics Laboratory (University of California at San Francisco) with data from the Brookhaven Protein Data Bank (Bolton & Perutz, 1970). We thank Professors Langridge and M. F. Perutz for their generous assistance.

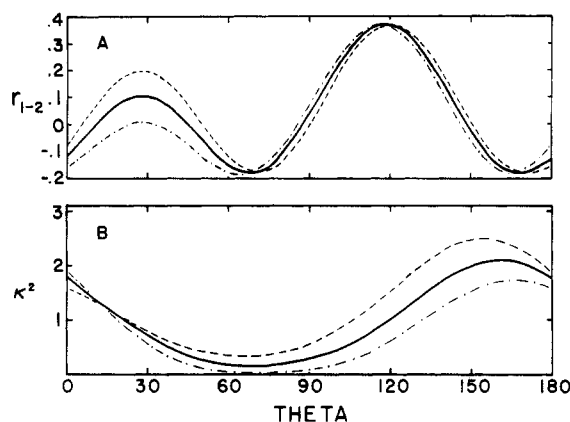


FIGURE 5: Calculated dependences for (A) the transfer anisotropy,  $r_{1-2}$ , and (B)  $\kappa^2$  on the transition dipole orientation,  $\theta$ , for  $\alpha_2^h(\text{deoxy})\beta_2^{\text{chl}}$ . The orientation of the chromophores is taken from the deoxy-Hb crystal structure;<sup>4</sup> see text. The experimentally determined value for  $r_{1-2}$  is  $0.10 \pm 0.03$ . The dashed lines indicate  $z = -5^\circ$ ; the dash/dot lines indicate  $z = +5^\circ$  (see text).

These values of  $r_{1-2}$  were calculated from a very slight modification of eq 2 which was required for consistency with the fact that the observed monomer anisotropy is not exactly  $2/5$  but rather  $r_0 = 0.374 \pm 0.004$ . In this modification a minor transition dipole moment with an amplitude 2% that of the principal transition dipole moment is included at an in-plane orientation perpendicular to  $\theta$  (which defines the orientation of the major dipole), and the transfer anisotropy is calculated as [see Appendix of Kuki & Boxer (1983)]

$$r_{1-2} = (2/5) \langle P_2(\hat{M}_1 \cdot \hat{M}_2) \rangle \quad (8)$$

The brackets denote a weighted average over interacting major and minor dipoles on the two fluorophores.

It is evident from Figure 5A that between one and four different values of  $\theta$  may give rise to the same value of  $r_{1-2}$ . With  $r_0 = 0.374 \pm 0.004$  and the observed  $r_\infty$ , we have  $r_{1-2} = 0.10 \pm 0.03$ . Using only the information in the  $r_\infty$  asymptote and the assumed structure, we can immediately restrict the possible values for  $\theta$  to the ranges  $18^\circ < \theta < 38^\circ$ ,  $92^\circ < \theta < 96^\circ$ , and  $141^\circ < \theta < 144^\circ$ . If we lift the restriction that the transition dipole must be *exactly* in the plane of the macrocycle determined by the deoxyhemoglobin crystal structure, we can arrive at one measure of the sensitivity of these conclusions to the assumption of exact homology in the chlorophyllide substitution. Additional curves were calculated for transition dipole orientations tipped  $\pm 5^\circ$  out of the plane from the position specified by  $\theta$  (Figure 5A). By use of these very reasonable bounds for the flexibility of the heme binding site,<sup>5</sup> the ranges of possible values for  $\theta$  expand to  $11^\circ < \theta < 46^\circ$ ,  $90^\circ < \theta < 97^\circ$ ,  $139^\circ < \theta < 146^\circ$ .

**Förster's Dipole-Dipole Theory.** The prediction of the Förster dipole-dipole excitation transfer theory (Förster, 1948) can be expressed as

$$k_t = (1/\tau_f)(R_0/R)^6[(3/2)\kappa^2] \quad (9)$$

where

$$R_0^6 = \frac{(3 \times 10^3)(\ln 10)c^4}{64\pi^5 n^4 N_{\text{av}}} (\eta_f) \int \frac{f_D(\nu)\epsilon_A(\nu)}{\nu^4} d\nu \quad (10)$$

<sup>5</sup> The issue of the flexibility of the heme binding site is not a question of dynamical fluctuations but rather of the range of probable equilibrium geometries for the large macrocycle. Heme disorder in reconstituted Hb has been observed (LaMar et al., 1978); the NMR spectra of the chlorophyllide-substituted hybrids analyzed here do not show any evidence of disorder in orientation about the macrocycle  $\alpha$ - $\gamma$  axis (Kuki & Boxer, 1983).

and

$$\kappa^2 = [\hat{M}_1 \cdot \hat{M}_2 - 3(\hat{M}_1 \cdot \hat{R})(\hat{M}_2 \cdot \hat{R})]^2 \quad (11)$$

$\tau_f$  is the singlet excited-state lifetime due to all deactivational processes other than the excitation transfer process in question,  $R$  is the interchromophore separation,  $\hat{R}$  is the corresponding unit vector, and  $\kappa$  is the orientation dependence of the dipole-dipole interaction energy. Equation 9 uses a dipole-dipole approximation to the interaction energy, and as such the center-to-center distance  $R$  is appropriate.  $f_D(\nu)$ ,  $\epsilon_A(\nu)$ ,  $\eta_f$ , and  $N_{\text{av}}$  are the corrected fluorescence spectrum normalized as  $\int f_D(\nu) d\nu = 1$ , the absorption spectrum in units of extinction coefficient per fluorophore, the observed fluorescence quantum yield in the absence of the acceptor, and Avogadro's number, respectively.  $n$  is the index of refraction, and the  $R_0$  values reported here are based on the index of refraction of the bulk sucrose solution,  $n = 1.36$  (see below for further discussion).

The calculated dependence of the  $\kappa^2$  term, which may range from zero to four, on the orientation  $\theta$  is shown in Figure 5B. Again we include curves calculated for transition dipoles tipped  $\pm 5^\circ$  out-of-plane for all values of  $\theta$ .<sup>6</sup>

**Value of  $R_0$ .** The value of the  $\kappa^2$  anisotropy factor cannot be immediately extracted from the observed excitation transfer rate constant  $k_t$  before a discussion of the value of the isotropic excitation transfer parameter,  $R_0$ . The Förster parameter  $R_0$  can be obtained either from an experimental study of truly randomly oriented molecules or from spectral parameters and eq 10. Studies on Rhodamine 6G in random solution have shown that the value of  $R_0$  calculated from the spectral overlap accurately reproduces the experimental value (Gochanour & Fayer, 1981). The calculated  $R_0$  for ZnPChla-ZnPChla excitation transfer in the  $\alpha_2^h(\text{deoxy})\beta_2^{\text{chl}}$  system is  $39.7 \pm 1.0 \text{ \AA}$ ; the principal sources of the uncertainty arise from the absolute fluorescence quantum yield and extinction coefficient. This value is significantly shorter than the  $R_0$  for ZnPChlaMb, which in turn is significantly shorter than that for chlorophyll *a* in ethyl ether (Knox, 1975; see Table I). Several factors are relevant here. The trivial factor is that the  $R_0$  value measures the excitation transfer rate *relative* to all other deactivational processes; since  $\tau_f$  is shorter for zinc than magnesium porphyrins, and  $\tau_f$  is further abbreviated in  $\alpha_2^h(\text{deoxy})\beta_2^{\text{chl}}$ , the corresponding  $R_0$  must be shorter simply to maintain the same actual transfer rate constant. To eliminate this effect, we present the values of  $R_0^6/\tau_f$ , which we will

<sup>6</sup> The higher transition multipole moments are commonly neglected when the fluorophores in question have strongly allowed dipole moments and when the interchromophore separation is several times the molecular diameter ( $\sim 5\times$  in our case). We have applied Chang's extended monopole method (1977) to the deoxy-Hb  $\beta$ - $\beta$  interchromophore geometry and obtain an estimated  $k_t$  which is 27% smaller than that based on the dipole-dipole approximation. We emphasize that this rather striking estimated difference is very sensitive to the mutual orientation of the two chromophores and to the transition monopole distribution within them. For example, the calculated monopole- and dipole-based transfer rates differ by less than 5% for *most* orientations at a 40.2- $\text{\AA}$  separation (provided that  $\kappa^2 > 0.1$ ). That the dipole-dipole approximation may need correction even at 40  $\text{\AA}$  can be understood by considering the next higher multipole interaction, which is the quadrupole-dipole. In the case of allowed dipole and quadrupole moments, we have  $k_t \propto (\kappa/R^3 + Q(\hat{M}_1, \hat{M}_2, \hat{R})/R^4)^2$ , where  $Q(\hat{M}_1, \hat{M}_2, \hat{R})$  is a quadrupole-dipole strength and orientation factor. The first term containing  $Q$  drops off as  $R^{-7}$ , so the ratio of this term to the dipole-dipole term drops off only as fast as  $R^{-1}$ . We caution, however, that the *quantitative* calculation of the correction is based on Chang's semiempirical wave functions for Chl *a* and that the *magnitudes and orientations* of the transition quadrupole moments are highly sensitive to the details of the wave functions. In the absence of firm evidence on these magnitudes and orientations, we have chosen not to include any estimated corrections in our analysis.

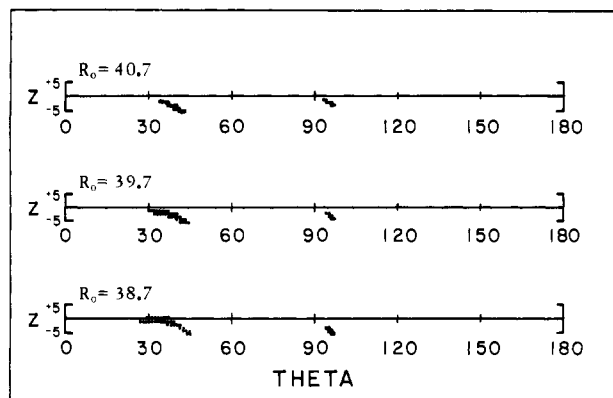


FIGURE 6: Mapping of the orientations of the  $S_1$  transition dipole moment which provide fits to the observed anisotropy decay for  $\alpha_2^h(\text{deoxy})\beta_2^{\text{Chl}}$ . The horizontal axis is the in-plane orientation,  $\theta$ , and the vertical axis is the out-of-plane component in degrees. The black areas indicate the deduced orientations (see text for fitting procedure). The  $R_0$  for this system is  $39.7 \pm 1.0$  Å. Note that the uncertainty in  $R_0$  has no significant effect on the ranges of  $\theta$  which fit the data.

call the isotropic excitation transfer coupling strength, in Table I.  $R_0^6/\tau_f$  is suitably independent of the rates of parallel nonradiative decay channels. We then find that the  $\alpha_2^h(\text{deoxy})\beta_2^{\text{Chl}}$  system exhibits an isotropic coupling strength of only 44% of the chlorophyll *a* value and ZnPChlaMb exhibits a coupling strength only slightly stronger at 56% of the chlorophyll *a* value. Thus, the rate of excitation transfer at any distance will be slower in these protein systems than would be predicted from the  $R_0$  value for chlorophyll *a* in organic solvent (ethyl ether).

The calculated isotropic coupling strength of the same chromophore in two different environments will vary if the natural radiative lifetime, the absorption dipole strength, the overlap of normalized absorption and emission band shapes, or the index of refraction differs in the two cases (eq 10). Previous investigations on the solution properties of chlorophyllide-substituted heme proteins (Boxer & Wright, 1979; Wright & Boxer, 1981; Kuki & Boxer, 1983) have shown that their absorption and emission spectra in the  $Q_Y$  region differ only slightly from the corresponding spectra of the chromophore in ethyl ether or methylene chloride.<sup>7</sup> The combination of the quantitative differences in extinction coefficient, band shapes, and natural radiative lifetimes, however, is sufficient to cause the factor of 2 reduction in the isotropic coupling strength, and hence in the expected excitation transfer rate constant. Such variations in the isotropic  $R_0^6/\tau_f$  should be expected in natural chlorophyll-containing proteins as well.

The index of refraction we have used in these calculations is that of the bulk solution and not some higher value that might be estimated for the index of refraction in the interior of the protein. The question of the appropriate index of refraction to use in the calculation of  $R_0$  in intraprotein excitation transport has not been previously resolved (Stryer, 1978; Dale & Eisinger, 1975). Various authors have employed different values, ranging from 1.33 to 1.5 (Fairclough & Cantor, 1978; Tao et al., 1983; O'Hara et al., 1981). We have analyzed this problem (see Appendix) and have concluded that the appropriate index of refraction to use is that of the bulk solution. This result is applicable to other cases of dilute solution intramolecular excitation transfer as well.

**Orientation of the Transition Dipole Moment.** The ZnPChla-ZnPChla excitation transfer rate constant at 40.2

Table III: Center-to-Center Interchromophore Separations for Deoxy-Hb<sup>a</sup>

$\alpha_1-\alpha_2$	34.8 Å	$\alpha_1-\beta_1$	36.4 Å
$\beta_1-\beta_2$	40.2 Å	$\alpha_1-\beta_2$	24.8 Å

Å is thus determined to be (using eq 9)  $k_1 = (3/2\kappa^2)[(6.5 \pm 1.0) \times 10^8] \text{ s}^{-1}$ . In combination with the calculated dependence of  $\kappa^2$  on  $\theta$  (Figure 5B), the rate constant  $k_1$  as a function of  $\theta$  is completely determined. The ranges of  $\theta$  which provide fits to the time-resolved anisotropy of  $\alpha_2^h(\text{deoxy})\beta_2^{\text{Chl}}$  are depicted in Figure 6. Also shown are the orientations,  $\theta$ , which fit the data provided that a  $z$  component of up to  $\pm 5^\circ$  is included. The region  $139^\circ < \theta < 146^\circ$  deduced from the consideration of  $r_\infty$  alone is eliminated while the two remaining possible ranges are narrowed. Note that the region  $93^\circ < \theta < 97^\circ$  is essentially consistent with the theoretical predictions. It is a coincidence that orientations of  $\theta \sim 36^\circ$  and  $\theta \sim 95^\circ$  possess both very similar dot products  $\hat{M}_1 \cdot \hat{M}_2$  and  $\kappa^2$  factors for the  $\alpha_2^h(\text{deoxy})\beta_2^{\text{Chl}}$  geometry and are thus indistinguishable on the basis of emission anisotropy measurements of this protein alone.

The  $\alpha_2^h\beta_2^h(\text{deoxy})$  system possesses a different relative geometry of the fluorescent macrocycles and thus offers a way to resolve the remaining ambiguity. The steady-state anisotropy of this protein is  $r = 0.289 \pm 0.005$  (Kuki & Boxer, 1983). From the spectral properties one obtains  $R_0 = 40.6 \pm 0.6$  Å. The steady-state anisotropy of the  $\alpha_2^h\beta_2^h(\text{deoxy})$  system is then calculated to be  $r = 0.285 \pm 0.008$  if  $\theta = 95^\circ \pm 2^\circ$ , or  $r = 0.289 \pm 0.055$  if  $z$  components of  $\pm 5^\circ$  are also included. On the other hand, if  $\theta = 36^\circ \pm 9^\circ$ , then the steady-state anisotropy would be  $r = 0.216 \pm 0.025$ , or if  $z = \pm 5^\circ$  is included,  $r = 0.216 \pm 0.052$ . Therefore, *only the orientation*  $\theta = 95^\circ \pm 2^\circ$  is consistent with the full set of anisotropy data measured in these chlorophyllide-substituted hybrids. This result is in accord with the predicted theoretical values near  $\theta = 90^\circ$  (Chang, 1977; Weiss, 1972; Petke et al., 1979).

**Abbreviated Fluorescence Lifetimes.** The fluorescence lifetimes of the  $\alpha_2^h\beta_2^{\text{Chl}}$  complex is markedly dependent on the state of oxidation and ligation of the heme iron (Table II). Evidently, the hemes in the  $\alpha$ -chains 25 Å (see Table III) from the chlorophyllides in the  $\beta$ -chains are not spectators but instead provide a pathway for the deactivation of the chlorophyllide singlet excited state. The relative triplet yields of ZnPChlaMb and  $\alpha_2^h(\text{deoxy})\beta_2^{\text{Chl}}$  have also been determined by separate transient absorption grating experiments [this method is described by von Jena & Lessing (1979) and Fayer (1982)]. The triplet yield of the former is 2.8 times that of the latter, which is exactly the ratio of their singlet lifetimes. This provides confirmation that a single new pathway exists for the deactivation of the  $S_1$  state of ZnPChla in  $\alpha_2^h(\text{deoxy})\beta_2^{\text{Chl}}$ , rather than a modification of the intersystem crossing rate constant.

We propose that the lifetime shortening is due to excitation transfer from the ZnPChla to low-lying excited states of the heme followed by rapid [ $\ll 1$  ps; see Adar et al. (1976)] dissipation by internal conversion in the heme. This interpretation is the only one consistent with all the lifetime data. The fluorescence lifetimes of ZnPChlaMb,  $\alpha_2^h\beta_2^{\text{Chl}}$ , and the methyl ester of ZnPChla in methanol are all in the range 3.7–4.0 ns. These are very typical values for zinc chlorins, and the polypeptide environment per se is evidently not a major perturbation. The fluorescence lifetime of  $\alpha_2^h(\text{deoxy})\beta_2^{\text{Chl}}$ , on the other hand, is  $1.42 \pm 0.05$  ns. As the tertiary and quaternary structures of  $\alpha_2^h\beta_2^{\text{Chl}}$  and  $\alpha_2^h(\text{deoxy})\beta_2^{\text{Chl}}$  appear to be very

<sup>7</sup> The circular dichroism spectra, on the other hand, are wholly altered when the chlorophyllides are inserted into the protein pockets.



similar (Kuki & Boxer, 1983), it is the presence of the heme in the ferrous deoxy state that is implicated.

The  $\alpha_2^h(\text{cyanomet})\beta_2^{\text{Chl}}$  hybrid exhibits a smaller though significant lifetime shortening, and this hexacoordinate ferric state may differ in tertiary and quaternary structure from the deoxy version. On the other hand, the hexacoordinate (and ferrous)  $\alpha_2^h(\text{carbonmonoxy})\beta_2^{\text{Chl}}$  hybrid exhibits a normal 3.75-ns lifetime. The distinguishing feature of the carbon monoxide ligated heme indeed appears to be neither its hexacoordination nor its ferrous state but rather its lack of very low-intensity and low-energy absorption features present in the deoxy and cyanomet forms.

Though the heme group has no strong absorption bands at longer wavelengths than 600 nm, lower energy excited states consisting of excitations of the iron d electrons or charge-transfer states nevertheless do exist. Some of these states in deoxy heme possess the quintuplet character of the ground state and are coupled to the ground state by weak transition dipoles as evidenced by the series of absorption bands ( $\epsilon < 1000 \text{ M}^{-1} \text{ cm}^{-1}$ ) extending from 600 to 910 nm (Eaton & Hofrichter, 1981). These low-energy states can accept the excitation of the ZnPChla through a dipole-dipole resonant excitation transfer mechanism. Excitation transfer by an exchange mechanism is conceivable, as the edge-to-edge interchromophore separation is less than  $25 \text{ \AA}$ .<sup>8</sup> However, the Förster  $R_0$  parameter for the ZnPChla to deoxy heme energy transfer is  $25.0 \pm 0.6 \text{ \AA}$ , as calculated by spectral overlap; thus, the dipole-dipole mechanism alone (e.g., with  $\kappa^2 = 1.1$ ) is quite sufficient to explain the observed lifetime abbreviation.

We note that the substantial impact that the state of a heme group  $25 \text{ \AA}$  away has on the chlorophyllide excited-state lifetime may have many naturally occurring analogues. Excitation transfer from antenna pigments to low-lying, weakly absorbing states of cytochromes occurring naturally in photosynthetic membranes may well limit the lifetime of the excited state within the antenna complex. Because these low-lying features depend strongly on redox potential and ligation, changes in fluorescence lifetimes observed during titrations may be the consequence of changes in the rate of this excitation trapping. Another potential excitation trap is provided by the broad, low-lying absorbance associated with chlorophyll anion and cation radicals in vitro and the radicals of various chlorophyll or pheophytin electron donors or acceptors in vivo. The extinction coefficients of these features in the relevant wavelength region are typically considerably larger than those for heme. Furthermore, the likely proximity of such anions and cations to the chromophore(s) whose lifetime is (are) being measured may allow very efficient excitation trapping (note that radical excited states are typically extremely short-lived). It is possible that such excitation trapping may explain the very short excited-state lifetimes of the primary electron donors in several species when the primary electron acceptor is reduced (Holten et al., 1978; Schenck et al., 1981).

## Conclusion

The observed migration of excitation energy within the chlorophyllide-substituted hemoglobin system can be completely and quantitatively explained by the use of Förster's resonant excitation transfer theory. In this system the depolarization of fluorescence is due to excitation transport between the chlorophyllides, while the lifetime shortening is due to excitation trapping by the lower energy heme states. From

a detailed analysis of the observed ZnPChla-to-ZnPChla excitation transfer rate constant, a  $Q_Y$  transition dipole orientation of  $\theta = 95 \pm 2^\circ$  relative to the molecular frame of the chlorophyllide is deduced. The analysis includes consideration of transition dipoles with out-of-plane components up to  $\pm 5^\circ$ . We do not know for certain whether or not the chlorophyllide may be rotated in-plane relative to the native heme but do not consider a substantial rotation to be likely in light of the considerable similarity in their molecular structures. However, it should be emphasized that the  $\theta$  value reported above is based on the assumption that the chlorophyllide replaces the heme substitutionally. This assumption will be checked when the necessary crystal structures are completed (Boxer et al., 1982).

## Appendix

The index of refraction that appears in Förster's equation (eq 10) has been consistently interpreted as the *index of refraction of the intervening medium* in previous discussions of intraprotein excitation transfer (Stryer, 1978; Dale & Eisinger, 1975; Fairclough & Cantor, 1978; Cantor & Schimmel, 1980). We will show that in fact the refractive index factor in Förster's equation is correctly interpreted as that of the bulk solution.

While the relation between the dielectric constant ( $\epsilon$ ) and the index of refraction,  $\epsilon = n^2$ , may be numerically valid for the frequencies of transitions considered here, the use of this relation in the derivation of eq 10 (Förster, 1948, 1965; Cantor & Schimmel, 1980) obscures the question at hand. Förster's equation has been derived for the case of a homogeneous dielectric. The case of dilute solution intraprotein excitation transfer is distinguished by its inhomogeneity. To a first-order approximation, we have an inhomogeneous dielectric consisting of a region surrounding the chromophore in which the local polarizable matter is very high in protein concentration and the bulk solution in which the protein concentration is very low. While there is no question that the intramolecular dipole-dipole energy should be attenuated by the dielectric constant appropriate for the immediate vicinity of the chromophores, this dielectric constant has *already been accounted for* by the use of experimentally determined extinction coefficients and radiative lifetimes. In fact the  $n^4$  factor appearing in eq 10 arises from the need to cancel extra factors implicit in the spectral overlap integral. Thus, the resolution of this question is obtained by examination of the dependences of the absorption cross-section and the Einstein  $A$  coefficient upon the dielectric constant and index of refraction.

The relevant equations for the extinction coefficient and Einstein  $A$  coefficient are (Dexter, 1953; Lax, 1952; Strickler & Berg, 1962)

$$\epsilon(\nu) = \frac{8\pi^3 N_{av}}{(3 \times 10^3)(\ln 10)hc} \left[ \frac{n}{\epsilon} \right] \mu^2(\nu) \quad (\text{A1})$$

and

$$A(\nu) = \frac{64\pi^4}{3hc^3} \left[ \frac{n^3}{\epsilon} \right] \nu^3 \mu^2(\nu) \quad (\text{A2})$$

where  $\mu^2(\nu)$  is the absolute square of the transition dipole matrix element including Franck-Condon factors. The essential feature is that in these equations, *as in the excitation transfer equations*, the  $\epsilon$  factor reflects predominantly the polarizability of the immediate protein environment which attenuates the electric fields at the site of the chromophore. It is evident that the product of the two spectral parameters above already contains the necessary  $\epsilon^{-2}$  factor. On the other hand, the index of refraction factor appears in eq A1 and A2

<sup>8</sup> Zemel & Hoffman (1981) have shown that an exchange mechanism did not participate during the *triplet lifetime* of the related zinc photoporphyrin IX substituted hemoglobin.

from a consideration of the density of final photon states and the macroscopic speed of light in the bulk solution. Equation 10, originally derived for homogeneous dielectrics, may thus be applied to dilute protein solutions by simply correcting for the  $n^4$  factor which reflects the average polarizability of the bulk solution. Dexter's derivation of eq 9 and 10 involves the same cancellation of the dielectric constant factor for the case of a homogeneous dielectric (Dexter, 1953). Dow has similarly argued that local field effects (which are not included here or by Dexter) are accounted for in the experimental determination of the spectral overlap integral (Dow, 1968).

The index of refraction of a dilute aqueous solution ( $n = 1.33$ ) is less than that appropriate for the interior of the protein ( $n \approx 1.5$ ), which can be estimated from the specific refractive index increment of hemoglobin [ $0.198 \text{ cm}^3 \text{ g}^{-1}$  (Sober, 1970)] by calculation of the protein's molecular polarizability. This latter value is appropriate if, for example, a solid crystal of the protein is under study. More commonly, the protein concentration is very dilute, and the use of the higher refractive index results in an underestimation of the excitation transfer rate constant. We conclude that, to a good approximation, the equation for  $R_0$  derived in the case of a homogeneous continuous dielectric is applicable to the case of dilute solution intramolecular excitation transfer provided that the absorption and emission spectra are recorded under the conditions of the energy-transfer measurement and the index of refraction of the bulk solution is employed.

**Registry No.** Zinc pyrochlorophyllide *a*, 41536-35-0.

## References

- Adar, F., Gouterman, M., & Aronowitz, S. (1976) *J. Phys. Chem.* **80**, 2184-2191.
- Albrecht, A. C. (1961) *J. Mol. Spectrosc.* **6**, 84-108.
- Bolton, W., & Perutz, M. F. (1970) *Nature (London)* **228**, 551.
- Boxer, S. G., & Wright, K. A. (1979) *J. Am. Chem. Soc.* **101**, 6791-6794.
- Boxer, S. G., Kuki, A., Wright, K. A., Katz, B. A., & Xuong, N. H. (1982) *Proc. Natl. Acad. Sci. U.S.A.* **79**, 1121-1125.
- Cantor, C. R., & Schimmel, P. R. (1980) *Biophysical Chemistry*, Vol. II, p 453, W. H. Freeman, San Francisco, CA.
- Chang, J. C. (1977) *J. Chem. Phys.* **67**, 3901-3909.
- Connolly, J. S., Janzen, A. F., & Samuel, E. B. (1982) *Photochem. Photobiol.* **36**, 559-563.
- Dale, R., & Eisinger, J. (1975) in *Biochemical Fluorescence Concepts* (Chen, R. F., & Edelhock, H., Eds.) Vol. I, pp 115-125, Marcel Dekker, New York.
- Dexter, D. L. (1953) *J. Chem. Phys.* **21**, 836-850.
- Dickerson, R. E., & Geis, I. (1969) *The Structure and Action of Proteins*, Harper & Row, New York.
- Dow, J. D. (1968) *Phys. Rev.* **174**, 962-976.
- Eaton, W. A., & Hofrichter, J. (1981) *Methods Enzymol.* **76**, 175-261.
- Ediger, M. D., Moog, R. S., Boxer, S. G., & Fayer, M. D. (1982) *Chem. Phys. Lett.* **88**, 123-127.
- Ediger, M. D., Dominique, R. P., & Fayer, M. D. (1984) *J. Chem. Phys.* (in press).
- Fairclough, R., & Cantor, C. R. (1978) *Methods Enzymol.* **48**, 347-379.
- Fayer, M. D. (1982) *Annu. Rev. Phys. Chem.* **33**, 63-87.
- Förster, Th. (1948) *Ann. Phys. (Leipzig)* **2**, 55-75.
- Förster, Th. (1965) in *Modern Quantum Chemistry* (Sinaoglu, O., Ed.) Vol. III, pp 93-137, Academic Press, New York.
- Gochanour, C. R., & Fayer, M. D. (1981) *J. Phys. Chem.* **85**, 1989-1994.
- Grinveld, A., & Steinberg, I. Z. (1974) *Anal. Biochem.* **59**, 583-598.
- Holten, D., Windsor, M. W., Parson, W. W., & Thornber, J. P. (1978) *Biochim. Biophys. Acta* **501**, 112-126.
- Jablonski, A. (1961) *Z. Naturforsch., A* **16A**, 1-4.
- Knox, R. S. (1975) in *Bioenergetics of Photosynthesis* (Govindjee, Ed.) pp 183-221, Academic Press, New York.
- Koglin, P. K. F., Miller, D. J., Steinwandell, J., & Hauser, M. (1981) *J. Phys. Chem.* **85**, 2363-2366.
- Kuki, A., & Boxer, S. G. (1983) *Biochemistry* **22**, 2923-2933.
- LaMar, G. N., Budd, D. L., Viscio, D. B., Smith, K. M., & Langry, K. C. (1978) *Proc. Natl. Acad. Sci. U.S.A.* **75**, 5755-5759.
- Lax, M. (1952) *J. Chem. Phys.* **20**, 1752-1760.
- Magde, D., Brannon, J. H., Cremers, T. L., & Olmsted, J. (1979) *J. Phys. Chem.* **83**, 696-699.
- McCalley, R. C., Shimschick, E. J., & McConnell, H. M. (1972) *Chem. Phys. Lett.* **13**, 115-119.
- Miller, R. J. D., Pierre, M., & Fayer, M. D. (1983) *J. Chem. Phys.* **78**, 5138-5146.
- Munro, I. H., & Sabersky, A. P. (1980) in *Synchrotron Radiation Research* (Winick, H., & Doniach, S., Eds.) pp 323-352, Plenum Press, New York.
- Munro, I. H., Pecht, I., & Stryer, L. A. (1979) *Proc. Natl. Acad. Sci. U.S.A.* **76**, 56-60.
- O'Hara, P., Yeh, S., Meares, C., & Bersohn, R. (1981) *Biochemistry* **20**, 4704-4708.
- Petke, J. D., Maggiora, G. M., Shipman, L. L., & Christoferson, R. E. (1979) *Photochem. Photobiol.* **30**, 203-223.
- Schenk, C. C., Parson, W. W., Holten, D., & Windsor, M. W. (1981) *Biochim. Biophys. Acta* **635**, 383-392.
- Seely, G. R. (1970) *J. Phys. Chem.* **74**, 219-227.
- Shragar, R. I. (1970) *J. Assoc. Comput. Mach.* **17**, 446-452.
- Sober, H. Ed. (1970) *Handbook of Biochemistry*, p C-68, Chemical Rubber Co., Detroit, MI.
- Song, P.-S., Moore, T. A., & Sun, M. (1972) in *Chemistry of Plant Pigments* (Chichester, C. O., Ed.) pp 33-74, Academic Press, New York.
- Strickler, S. J., & Berg, R. A. (1962) *J. Chem. Phys.* **37**, 814-822.
- Stryer, L. (1978) *Annu. Rev. Biochem.* **47**, 819-846.
- Stryer, L., & Haugland, R. P. (1967) *Proc. Natl. Acad. Sci. U.S.A.* **58**, 719-726.
- Tao, T. (1969) *Biopolymers* **8**, 609-632.
- Tao, T., Lamkin, M., & Lehrer, S. S. (1983) *Biochemistry* **22**, 3059-3066.
- Trosper, T., Park, R. B., & Sauer, K. (1968) *Photochem. Photobiol.* **7**, 451-469.
- Tweet, A. G., Bellamy, W. D., & Gaines, G. L. (1964) *J. Chem. Phys.* **41**, 2068-2077.
- Von Jena, A., & Lessing, H. E. (1979) *Opt. Quantum Electron.* **11**, 419-439.
- Weiss, C. (1972) *J. Mol. Spectrosc.* **44**, 37-80.
- Wright, K. A., & Boxer, S. G. (1981) *Biochemistry* **20**, 7546-7556.
- Zemel, H., & Hoffman, B. M. (1981) *J. Am. Chem. Soc.* **103**, 1192-1201.